γ-ray multipolarimetry between low-spin states of ^{136}Ce: Search for the $2^+_{1,\mathrm{ms}}$ one-phonon mixed-symmetry state

T. Ahn,[1,2,3] N. Pietralla,[1,2,3] G. Rainovski,[1,4] A. Costin,[1,2,3] K. Dusling,[1] T. C. Li,[1] A. Linnemann,[2] and S. Pontillo[1]
[1]*Department of Physics and Astronomy, State University of New York at Stony Brook, Stony Brook, New York 11794-3800, USA*
[2]*Institut für Kernphysik, Universität zu Köln, D-50937 Köln, Germany*
[3]*Institut für Kernphysik, Technische Universität Darmstadt, D-64289 Darmstadt, Germany*
[4]*Faculty of Physics, St. Kliment Ohridski University of Sofia, Sofia 1164, Bulgaria*
(Received 9 June 2006; published 24 January 2007)

An experiment was performed on ^{136}Ce to measure $E2/M1$ multipole mixing ratios using the method of $\gamma\gamma$ angular correlations. The low-spin states of interest were populated by β decay from the 2^+ ground state of ^{136}Pr that has a half-life of 13.1 min. Emitted γ rays were detected with the Stony Brook cube germanium detector array. Five $E2/M1$ multipole mixing ratios were measured for the first time and two spin and parity quantum numbers were assigned. Candidates for the $2^+_{1,\mathrm{ms}}$ state of ^{136}Ce were identified from large $M1$ fractions in the $E2/M1$ multipole mixing ratios. The $2^+_{1,\mathrm{ms}}$ state is suggested to be fragmented between the closely lying 2^+_3 and 2^+_4 states. A two state mixing scenario is employed for deducing an F-spin mixing matrix element of 43(5) keV.

DOI: 10.1103/PhysRevC.75.014313 PACS number(s): 21.10.Re, 23.20.En, 23.20.Gq, 27.60.+j

I. INTRODUCTION

Proton-neutron mixed-symmetry states arise from the Interacting Boson Model-2 (IBM-2) where in the model valence particles couple to form proton and neutron pairs and these pairs are approximated as bosons [1,2]. In the IBM-2, the proton-neutron symmetry of wave functions can be quantified by the F-spin quantum number [3]. F-spin is an analog to nucleon isospin for proton and neutron bosons. Proton bosons and neutron bosons form an F-spin doublet. Conventionally, proton bosons are assigned the projection $F_z = +1/2$, while neutron bosons have $F_z = -1/2$. Multiboson wave functions formed by N_π proton bosons and N_ν neutron bosons can be coupled to good total F-spin. States with F-spin at its maximal value, $F_{\max} = (N_\pi + N_\nu)/2$, are called fully-symmetric states whereas states with F-spin less than the maximal value are called mixed-symmetry states. The properties of mixed-symmetry states can test parts of the IBM-2 Hamiltonian, which the fully-symmetric states are insensitive to, e.g., the Majorana operator. Many numerical studies of nuclear properties in the framework of the IBM-2 make use of Talmi's Hamiltonian [2]

$$H = \epsilon\left(n_{d_\pi} + n_{d_\nu}\right) + \kappa Q^\chi_\pi \cdot Q^\chi_\nu + \lambda \hat{M}, \qquad (1)$$

where n_{d_π} (n_{d_ν}) is the number of proton (neutron) d-bosons; Q_π (Q_ν) is the proton (neutron) quadrupole operator; $\hat{M}$ is the Majorana operator; and ϵ, κ, χ, and λ are model parameters. For realistic parameter values F-spin is an approximate quantum number for the eigenstates of this Hamiltoninan.

The 1^+_{sc} mixed-symmetry state found in deformed nuclei, also known as the scissors mode, was first discovered in ^{156}Gd by Bohle *et al*. [4]. The one-phonon $2^+_{1,\mathrm{ms}}$ state was suggested experimentally by Hamilton, Irbäck, and Elliott [5], and $2^+_{1,\mathrm{ms}}$ one-phonon and two-phonon mixed-symmetry states in near-spherical nuclei have been found more recently in the $A = 90$ region (e.g., Refs. [6,7]) and the $A = 130$ region (e.g., Refs. [8–11]). These data show that the $2^+_{1,\mathrm{ms}}$ acts as a building block of nuclear structure.

The signature of the $2^+_{1,\mathrm{ms}}$ mixed-symmetry state is a strong $M1$ transition to the 2^+_1 state and a weakly collective $E2$ decay to the 0^+_1 ground state [12]. The measurement of multipole mixing ratios is needed for $M1$ transition strengths to be extracted from decay rates. One method that can be used for measuring γ-ray multipole mixing ratios is through a $\gamma\gamma$ angular correlation measurement. This method has been used previously to identify candidates for mixed-symmetry states [5,13]. Firm assignments of mixed-symmetry states require knowledge of absolute transition rates.

Recently, a measurement of transition matrix elements was done for the $A = 138$ nuclide ^{138}Ce, which yielded the identification of the $2^+_{1,\mathrm{ms}}$ mixed-symmetry state of that nucleus [14]. Also in ^{142}Ce, the $2^+_{1,\mathrm{ms}}$ has been found on the other side of the $N = 82$ shell closure [10]. It is interesting to look at the Ce isotopes because they are at the $\pi g_{7/2}$ sub-shell closure and mixed-symmetry states show a sensitivity to this [14]. The aim of this article is to present the results of the measurement of $E2/M1$ multipole mixing ratios and from them propose a candidate for the $2^+_{1,\mathrm{ms}}$ one-phonon mixed-symmetry state of ^{136}Ce. In the following section, experimental procedure and equipment are described. In Sec. III, the results of the angular correlation data analysis are presented. This includes five previously unknown $E2/M1$ multipole mixing ratios and two spin and parity assignments. In Sec. IV, the experimental results are discussed in relation to the low-spin level schemes of neighboring even-even Ce isotopes and $N = 78$ isotones. Finally, a two-state mixing scenario is used for estimating the size of the F-spin mixing matrix element in ^{136}Ce from the observed $E2/M1$ multipole mixing ratios. A conclusion is presented in Sec. V.

II. EXPERIMENT

The states of interest in ^{136}Ce were populated using the EC/β^+ decay of the 2^+ state of ^{136}Pr, which has a half-life of 13.1 min. The mother nuclei of ^{136}Pr were produced using the ^{134}Ba(^{6}Li, 4n)^{136}Pr fusion evaporation reaction where a ^{6}Li beam was accelerated to an energy of 47 MeV using the FN-Tandem Van de Graaff and superconducting LINAC accelerators at the Nuclear Structure Laboratory at SUNY at Stony Brook. Two targets of ^{134}Ba in the form of barium carbonate with a thickness of approximately 18 mg/cm^2 were used.

Each target was alternately irradiated in an irradiation chamber for 30 min at a time, which is approximately two half-lives of the ^{136}Pr 2^+ state. The irradiated target was then placed into the target chamber of the Stony Brook Cube array [15]. Two targets were used so that one could be irradiated and one could be placed in the Stony Brook Cube array for the measurement of γ-rays. The two targets were swapped at 30-min intervals. This allowed the detector array to always have a sufficiently active source in its chamber that resulted in an initial coincidence counting rate of about 1000 Hz, which decreased to about 400 Hz after the 30-min interval. The Stony Brook Cube array consisted of six coaxial high-purity Ge detectors. Each of the detectors had an efficiency of 30% relative to the NaI detector standard. Data were taken for $\gamma\gamma$ coincidences for a period of 40 h. After the data from the ^{136}Pr β decay were taken, energy and efficiency calibrations were done using a ^{152}Eu and ^{56}Co source. After analog-to-digital conversion, all data were written directly to computer hard disk for off-line analysis.

The Stony Brook Cube array has a cubical target chamber, which has collimation for the faces and corners of the cube [15]. Five detectors were positioned in front of the faces of the cube chamber while one was positioned to face one corner. This allowed us to form three coincidence groups, where each group was composed of pairs of detectors and defined by the relative angle between each pair. Pairs of detectors in Group 1 had a 90° relative angle, pairs in Group 2 had a 180° relative angle, and pairs in Group 3 had either a 54.7° or a $\pi - 54.7° = 125.3°$ relative angle. The number of pairs in Groups 1, 2, and 3 were eight, two, and five, respectively.

The data were sorted off-line into three symmetric E_γ-E_γ matrices, one corresponding to each of the three detector groups. A total of 1.1×10^8 $\gamma\gamma$ coincidences were sorted. A sample projection for the Group 1 matrix is shown in Fig. 1.

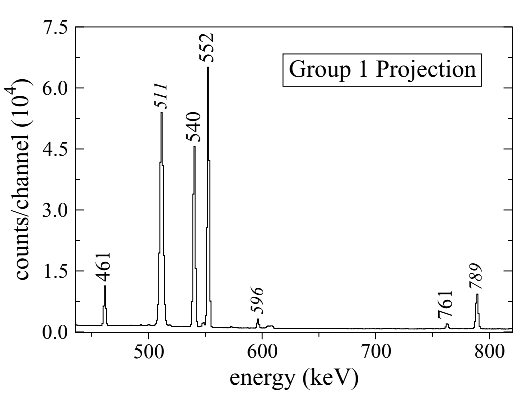

FIG. 1. The γ-ray spectrum observed from the ^{136}Pr β decay. Displayed is the lower energy portion of the $\gamma\gamma$ coincidence matrix projection observed with Ge detectors at a relative angle of 90° (Group 1).

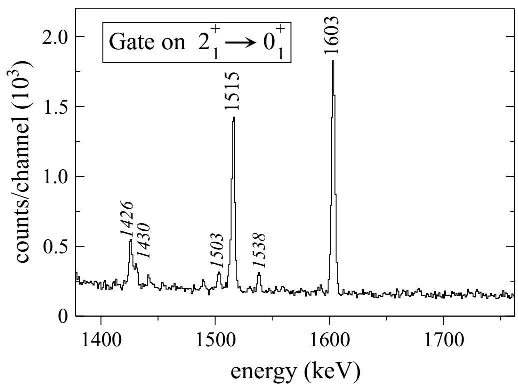

FIG. 2. The γ-ray spectrum observed from the ^{136}Pr β decay. Displayed is one energy region of interest in the coincidence spectrum gated on the 552-keV ($2_1^+ \rightarrow 0_1^+$) transition for Ge detectors at a relative angle of 90° (Group 1).

The 552-, 540-, 461-, and 761-keV transitions, which are from the decay of excited states in ^{136}Ce, can be seen. A coincidence spectrum gated on the 552-keV ($2_1^+ \rightarrow 0_1^+$) transition is shown in Fig. 2. The peaks corresponding to transitions connecting the 2_4^+ and 2_3^+ states with the 2_1^+ state at energies of 1515 keV and 1603 keV, respectively, can be seen. A partial level scheme for ^{136}Ce including the γ-ray transitions for which we could perform $\gamma\gamma$ angular correlation analysis is shown in Fig. 3.

III. DATA ANALYSIS AND RESULTS

The angular correlation function, $W(\theta)$, gives the coincidence intensity of two γ rays emitted in a cascade from an initially unoriented source as a function of the angle θ between them. The theoretical description of angular correlations for unoriented sources is given in Ref. [16]. $W(\theta)$ can be expressed as an expansion in Legendre polynomials,

$$W(\theta) = A_0 + A_2 P_2(\cos\theta) + A_4 P_4(\cos\theta) + \cdots \quad (2)$$

$$= A_0[1 + a_2(\delta_1, \delta_2)P_2(\cos\theta) + a_4(\delta_1, \delta_2)P_4(\cos\theta) + \cdots], \quad (3)$$

where A_0 is the total coincidence intensity and $a_2 = A_2/A_0$ and $a_4 = A_4/A_0$ are the normalized angular correlation coefficients. Only even terms appear and, for the transitions

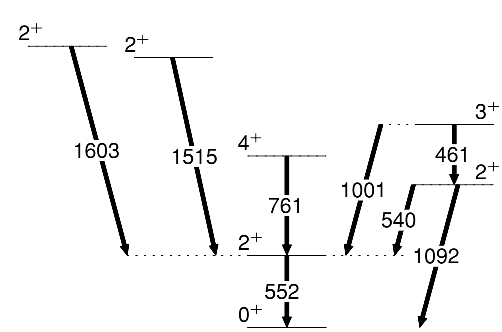

FIG. 3. Partial level scheme for ^{136}Ce showing relevant low-spin states populated by β decay and the transitions for which angular correlation analysis could be done.

that we have studied, only terms up to the $P_4(\cos\theta)$ term are needed.

The coincidence intensities were measured by gating on one of the γ rays in a cascade and measuring the area of the peak corresponding to the second γ ray in the gated spectrum. This area was then corrected for the relative efficiency of the detectors and the number of detector pairs in the group. The group matrix defines the angle at which the intensity was measured.

Generally, the a_2 and a_4 coefficients are functions of the multipole mixing ratios δ_1 and δ_2 of the first and second transitions, respectively. The definition of δ we use is given by

$$\delta = \frac{\sqrt{3}}{10}\frac{E_\gamma}{\hbar c}\frac{\langle \Psi_f \| E2 \| \Psi_i \rangle_{\rm BM}}{\langle \Psi_f \| M1 \| \Psi_i \rangle_{\rm BM}}, \tag{4}$$

which follows from Eq. (6) from Ref. [17]. The reduced transition matrix elements are those given by Bohr and Mottelson [18]. With this definition of δ, the a_2 and a_4 coefficients are given by

$$a_n = b_n(\gamma_1)c_n(\gamma_2) \tag{5}$$

with

$$b_n(\gamma_1) = \frac{1}{1+\delta_1^2}[F_n(L_1, L_1, J_i, J) - 2\delta_1 F_n(L_1, L_1', J_i, J) + \delta_1^2 F_n(L_1', L_1', J_i, J)] \tag{6}$$

and

$$c_n(\gamma_2) = \frac{1}{1+\delta_2^2}[F_n(L_2, L_2, J_f, J) + 2\delta_2 F_n(L_2, L_2', J_f, J) + \delta_2^2 F_n(L_2', L_2', J_f, J)], \tag{7}$$

where n is an index with values 2 or 4; J_i, J, and J_f are the spins of the initial, intermediate, and final states, respectively; L, L' are the leading and next-to-leading γ-ray multipolarities; and $F_n(L, L', J_i, J)$ are the F coefficients, which are tabulated in several references [16,19,20].

The program CORLEONE [21,22] was used to fit the angular correlation functions to the measured intensities. The best A_0, A_2, and A_4 coefficients were found using a χ^2-minimization fit with respect to the variable δ_1 for a given spin hypothesis for J_i. The values for J and J_f were already known for the cascades that we studied. The second transition consisted of a decay from a 2^+ state to the 0^+ ground state, which is of pure $E2$ character. Thus for all cascades analyzed, δ_2 was set to zero. To determine the correct group efficiencies, group intensities were fixed to the (761–552)-keV cascade, which has a known spin sequence of 4-2-0. The second and third group intensities were renormalized by factors of 1.07(4) and 1.21(3), respectively, to obtain a δ_1 value equal to zero.

A plot of fits to the data for several hypotheses for J_i for the (1603–552)-keV cascade is shown in Fig. 4. It can be seen that the fit for the 2-2-0 spin sequence fits the data well while the fits for both the 3-2-0 and 1-2-0 spin sequences fail to fit the data. This is also reflected in the resulting reduced χ^2 from the fits, with the 3-2-0 and 1-2-0 spin sequences resulting in large reduced χ^2 values. The hypotheses for J_i that yielded large reduced χ^2 were rejected as probable values.

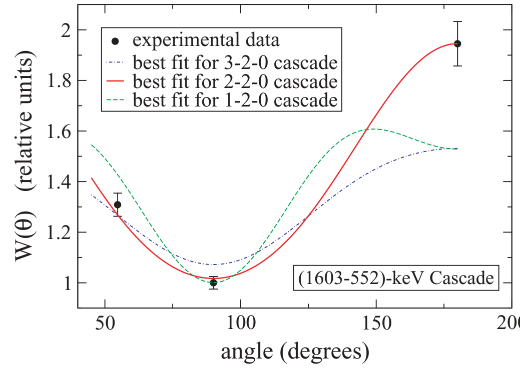

FIG. 4. (Color online) Angular correlation functions fitted to data for 3-2-0, 2-2-0, and 1-2-0 spin hypotheses with the $E2/M1$ multipole mixing ratio for the preceding transition, δ_1, treated as a free parameter in each case.

Each fit also yielded a δ_1 value for which the χ^2 was a minimum. Another way to visualize the best fit δ_1 values is to plot parametrically a_2 and a_4 as a function of a full range of possible δ_1 values for a given spin sequence and also plot the experimentally measured a_2 and a_4 values for a given cascade. Plots for the possible 4-2-0, 3-2-0, 2-2-0, and 1-2-0 spin sequences, as well as the data for the five cascades that were studied, are shown in Fig. 5. It can be seen that three of the points fall on the plot for the 2-2-0 cascade within the error bars while two others lie on or are close to the 3-2-0 as well as the 1-2-0 spin sequence plots. The three levels from which the (1603–552)-, (1515–552)-, and (540–552)-keV cascades originate were assigned to have $J_i = 2$. The two other points, the ones for the (461–1092)-keV and (1001–552)-keV cascades, both originate from the same state, and

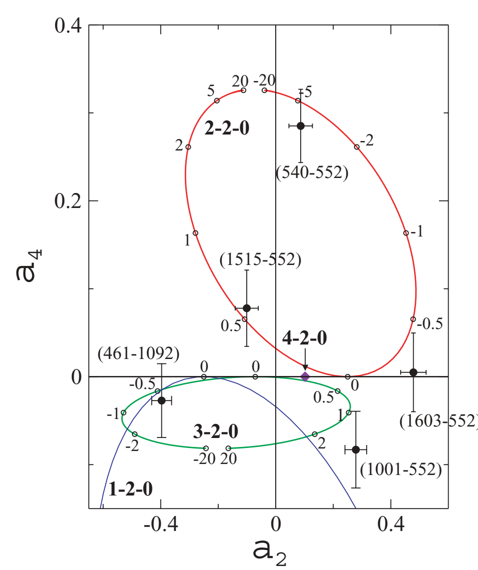

FIG. 5. (Color online) The theoretical ellipses for the a_2 and a_4 angular correlation coefficients plotted parametrically as functions of δ_1 for quadrupole-dipole mixing are shown along with the data (filled circles) for the (552–540)-, (552–1515)-, (552–1603)-, (461–1092)-, and (1001–552)-keV cascades. Values of δ_1 on the ellipses are denoted with open circles.

TABLE I. Measured $E2/M1$ multipole mixing ratios, δ_1, and fractional $E2$ contribution for corresponding transitions and spin sequences.

Cascade (keV)	Spin sequence	δ_1	$E2$ fraction
(540–552)	$2_2^+ \to 2_1^+ \to 0_1^+$	−4.7(7)	0.96(1)
(1001–552)	$3_1^+ \to 2_1^+ \to 0_1^{+a}$	0.97(28)	0.48(14)
(461–1092)	$3_1^+ \to 2_2^+ \to 0_1^{+a}$	−0.50(4), −4.3(6)	0.20(3), 0.95(1)
(1515–552)	$2_3^+ \to 2_1^+ \to 0_1^{+a,b}$	0.46(8)	0.17(5)
(1603–552)	$2_4^+ \to 2_1^+ \to 0_1^{+b}$	−0.41(8)	0.14(5)

[a]New spin assignment for J_i.
[b]New parity assignment for J_i^π.

a spin assignment of $J_i = 1$ or $J_i = 3$ is possible. We favor $J_i = 3$ because of the fact that we do not observe a direct transition from this state to the ground state, which is also noted in Ref. [23]. The results from the fits are tabulated in Table I. Positive parities were assigned to all states observed because of the values of δ_1 significantly differing from zero and such a value is highly unlikely for a fast $M2/E1$ mixed transition. $E2$ fractions, which are given by $\delta^2/1+\delta^2$, were calculated from the fitted δ_1 values. The decays from the 2_3^+ and 2_4^+ states clearly have a significant $M1$ contribution.

IV. DISCUSSION

First, the 540-keV transition has a very large $E2$ fraction of 96(1)%. This supports that the 2_2^+ state at 1092 keV from which the 540-keV transition originates can be interpreted as the 2^+ member of the two-phonon fully-symmetric triplet. It is at nearly twice the excitation energy of the 2_1^+ state, which is also expected for a two-phonon state. Final proof for its symmetric two-phonon character can only come from the measurement of the $B(E2; 2_2^+ \to 2_1^+)$ value.

Second, it can be seen that the first transitions in the (1515–552)-keV and (1603–552)-keV cascades have an $E2$ fraction of 0.17(5) and 0.14(5), respectively. This means over 80% of their transition intensities comes from $M1$ contribution. One possible source for sizable $M1$ transition strengths between low-energy, low-spin states is from the mixed-symmetry character of their wave functions. The 2067- and 2155-keV states, which are the initial states of the (1515–552)- and (1603–552)-keV cascades, respectively, are candidates for the $2_{1,\mathrm{ms}}^+$ in ^{136}Ce. Because both $E2/M1$ multipole mixing ratios indicate dominant $M1$ character, the $2_{1,\mathrm{ms}}^+$ state may be fragmented over the 2_3^+ and 2_4^+ states as it has been the case in the neighboring isotope ^{138}Ce [14]. The following discussion focuses on the arguments that favor this interpretation.

A. Comparison of Ce isotopes

The energy levels of ^{136}Ce and its neighboring even-even isotopes ^{134}Ce and ^{138}Ce are shown in Fig. 6. Only positive parity states are plotted for clarity. Additionally for ^{134}Ce, only states with $J < 4$ excluding the 4_1^+ are plotted. The decreasing energies of the 2_1^+ states with increasing distance from the $N = 82$ neutron shell closure show an increasing collectivity. The 2_2^+ states also decrease in energy, keeping in line with being roughly at twice the excitation energy of the 2_1^+. In the isotope ^{138}Ce, the 2_2^+ state has recently been measured to decay by a 80(5)% $E2$ fraction to the 2_1^+ state with a strength of $B(E2; 2_2^+ \to 2_1^+) = 28(2)$ W.u., thereby clearly demonstrating its symmetric two-phonon character. Furthermore, the $2_{3,4}^+$ states of ^{138}Ce at around 2200 keV are known to be the fragmented $2_{1,\mathrm{ms}}^+$ state with an F-spin mixing matrix element of $V(^{138}\mathrm{Ce}) = 44(3)(^{+3}_{-14})$ keV, where the first set of parentheses gives the statistical uncertainty and the second the systematical errors [14]. These closely lying $2_{3,4}^+$ states show much similarity to the $2_{3,4}^+$ states in ^{136}Ce that are proposed to be the fragmented $2_{1,\mathrm{ms}}^+$ state because of their small $E2/M1$ multipole mixing ratios. For ^{134}Ce, there is similarity with ^{136}Ce in the energy levels up to about 1500 keV. However, recent studies of ^{134}Ce low-spin levels [24] do not show any evidence for fragments of the $2_{1,\mathrm{ms}}^+$ state below 2000 keV.

B. $N = 78$ isotones

The comparison of the energy levels of the $N = 78$ isotones ^{134}Ba and ^{136}Ce is shown in Fig. 7. Again only positive parity states are shown for clarity. There is a clear similarity in the structures of both isotopes up to around 2100 keV that is even more so than for the Ce isotopes, perhaps due to the similar

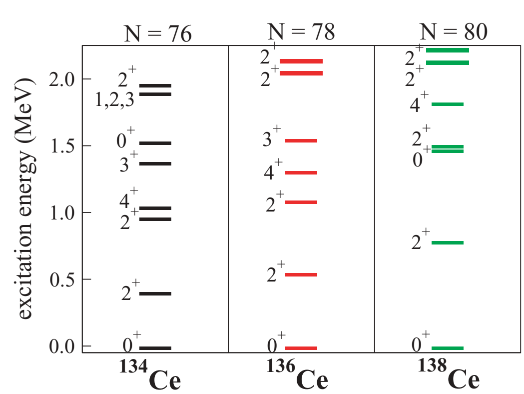

FIG. 6. (Color online) Comparison of energy levels in Ce isotopes. The larger lines represent the candidates for the fragmented $2_{1,\mathrm{ms}}^+$ state in ^{136}Ce and the fragmented $2_{1,\mathrm{ms}}^+$ state in ^{138}Ce.

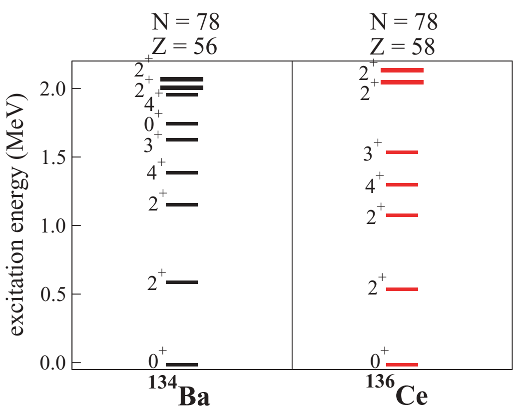

FIG. 7. (Color online) Comparison of the low-energy level schemes of the $N = 78$ isotones, ^{134}Ba and ^{136}Ce. The larger lines represent the fragmented $2^+_{1,\mathrm{ms}}$ state of ^{134}Ba and the proposed candidates for the fragmented $2^+_{1,\mathrm{ms}}$ state of ^{136}Ce.

deformation of the two isotones. The β values for the two isotones are $\beta(^{134}\mathrm{Ba}) = 0.1609(9)$ and $\beta(^{136}\mathrm{Ce}) = 0.170(9)$ [25]. The $2^+_{1,\mathrm{ms}}$ mixed-symmetry state has also been found in ^{134}Ba and it is again known to be fragmented over the two closely lying $2^+_{3,4}$ states at around 2100 keV [9]. These two states have $B(M1)$ values of 0.062(8) μ_N^2 and 0.137(12) μ_N^2 for the 2^+_3 and 2^+_4 states, respectively, which is evidence for the presence of a $2^+_{1,\mathrm{ms}}$ state at a mean energy of $E(2^+_{1,\mathrm{ms}}) =$ 2070(2) keV when weighted by the $M1$ transition strengths. This similarity further supports the conjecture that the $2^+_{1,\mathrm{ms}}$ mixed-symmetry state of ^{136}Ce is also fragmented over the 2^+_3 and 2^+_4 states at 2067 and 2155 keV.

C. Two state mixing

Our experimental findings in ^{136}Ce and the shown systematics suggest that the 2^+_3 and 2^+_4 states in ^{136}Ce are a mixture of the $2^+_{1,\mathrm{ms}}$ and a closely lying fully-symmetric state. This mixing can be considered in a two-state mixing scenario, the rationale of which is illustrated in Fig. 8. We assume that the unmixed picture corresponds to the F-spin limit of the IBM-2. Hence, there is no $M1$ transition between a 2^+_f fully-symmetric state and the 2^+_1 state. From this scheme, the 2^+_3 and 2^+_4 states can be expressed as

$$|2^+_4\rangle = \alpha|2^+_{1,\mathrm{ms}}\rangle + \beta|2^+_f\rangle, \tag{8}$$

$$|2^+_3\rangle = -\beta|2^+_{1,\mathrm{ms}}\rangle + \alpha|2^+_f\rangle, \tag{9}$$

where the coefficients α and β are written such that the 2^+_3 and the 2^+_4 states are orthogonal. An elementary treatment of the two-state mixing scenario yields

$$E_f + E_{1,\mathrm{ms}} = E(2^+_3) + E(2^+_4) \tag{10}$$

and

$$E_{1,\mathrm{ms}} = \frac{E(2^+_4) + r^2 E(2^+_3)}{1 + r^2}, \tag{11}$$

where E_f and $E_{1,\mathrm{ms}}$ are the unperturbed energies and where we define the positive ratio $r \equiv \frac{\beta}{\alpha}$. The F-spin mixing matrix element between the two states is given by

$$V = r[E(2^+_4) - E_f]. \tag{12}$$

The unperturbed energies and the size of the perturbation can be obtained from these equations if the ratio of mixing amplitudes r could be estimated. The observed $E2/M1$ multipole mixing ratios contain information on this ratio because the $M1$ strengths are generated from the $2^+_{1,\mathrm{ms}}$ mixed-symmetry basis state only. Using Eq. (4) this two state mixing scenario yields

$$\frac{\delta_{2^+_4\to 2^+_1}}{\delta_{2^+_3\to 2^+_1}} = \frac{E_\gamma(2^+_4 \to 2^+_1)}{E_\gamma(2^+_3 \to 2^+_1)} \frac{q + r}{q - \frac{1}{r}}, \tag{13}$$

where we define q as

$$q \equiv \frac{\langle 2^+_1 \| E2 \| 2^+_{1,\mathrm{ms}}\rangle}{\langle 2^+_1 \| E2 \| 2^+_f\rangle} \tag{14}$$

and where we have used the fact that $\langle 2^+_1 \| M1 \| 2^+_f\rangle$ equals zero due to F-spin selection rules because both basis states, 2^+_1 and 2^+_f, are fully-symmetric states.

To estimate r, we must make an assumption on q, the ratio of $E2$ matrix elements from the unperturbed states to the 2^+_1 state. It is assumed that the 2^+_f state is a predominantly three-phonon state with minor two-phonon or four-phonon components. For nuclei with O(5) symmetry, the numerator of Eq. (14) is zero because of d-parity selection rules [26] in the consistent Q formalism. Indeed, it has previously been observed that the $E2$ transition strength from the one-phonon $2^+_{1,\mathrm{ms}}$ state to the symmetric one-phonon 2^+_1 state is typically much smaller than allowed $E2$ strengths between fully-symmetric states [6]. Therefore, it is reasonable to expect $q \ll 1$.

Because ^{136}Ce is a vibrational nucleus we consider the d-parity selection rules to be well fulfilled. Assuming $q = 0$, Eq. (13) simplifies to

$$\frac{\delta_{2^+_4\to 2^+_1}}{\delta_{2^+_3\to 2^+_1}} \approx -\frac{E_\gamma(2^+_4 \to 2^+_1)}{E_\gamma(2^+_3 \to 2^+_1)} r^2. \tag{15}$$

Note that the two-state mixing scenario requires opposite signs for the $E2/M1$ multipole mixing ratios for these two strongly

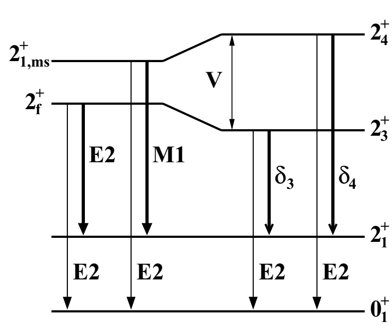

FIG. 8. Schematic of a two-state mixing scenario for the $2^+_{1,\mathrm{ms}}$ mixed-symmetry state and a 2^+_f fully-symmetric state.

mixed states. This is indeed what we observed, which indicates support for our analysis. Equation (15) then yields

$$r \approx \sqrt{-\frac{\delta_{2_4^+\to 2_1^+}}{\delta_{2_3^+\to 2_1^+}} \frac{E_\gamma(2_3^+ \to 2_1^+)}{E_\gamma(2_4^+ \to 2_1^+)}} = 0.92(11). \tag{16}$$

The similarity of the absolute values of the observed $E2/M1$ multipole mixing ratios $\delta_{2_3^+\to 2_1^+} = 0.46(8)$ and $\delta_{2_4^+\to 2_1^+} = -0.41(8)$ suggest strong mixing with mixing amplitudes α and β having the same order of magnitude, i.e., $r \approx 1$. From the result of Eq. (16), the mixing amplitudes follow to be $\alpha = 0.74(4)$ and $\beta = 0.67(9)$. Equations (10)–(12) yield values of $E_f = 2108$ keV and $E_{1,\mathrm{ms}} = 2114$ keV for the initial unperturbed energies and $V = 43(5)$ keV.

It is remarkable that this estimate of $V = 43(5)$ keV agrees with the recently measured value of $V(^{138}\mathrm{Ce}) = 44(3)(^{+3}_{-14})$ keV for the neighboring isotope ^{138}Ce [14]. In contrast to the present approach, the value for $V(^{138}\mathrm{Ce})$ was obtained unambiguously from absolute $M1$ transition strengths. The striking equality of observed F-spin mixing matrix elements $V_{F-\mathrm{mix}} \approx 44$ keV in the ^{136,138}Ce isotopes shows that this interaction is independent of neutron number in this mass region where valence neutrons occupy the $1h_{11/2}$ orbit. On the contrary, this observation strongly supports the interpretation that the presence of the $\pi(g_{9/2}$ sub-shell closure at $Z = 58$ (Ce) dominates the F-spin breaking as it has been demonstrated for the $N = 80$ isotones ^{138}Ce and ^{136}Ba [14].

Now we address the consistency of the two-state mixing scenario with decay data on the $2_{3,4}^+$ states. The branching ratios measured in the literature for transitions coming from the 2_3^+ and 2_4^+ states differ substantially [23]. The 2_4^+ state decays predominantly to the 2_1^+ state while the decay of the 2_3^+ state decays more strongly to the 0_1^+ ground state. Using the information that is available from the published branching ratios and our measured multipole mixing ratios, it is desirable to estimate what the possible ratio of $E2$ transition matrix elements from the 2_3^+ and 2_4^+ state to the ground state would be. Defining the $E2$ matrix elements for transitions from the unperturbed $2_{1,\mathrm{ms}}^+$ and 2_f^+ states to the ground state as $\epsilon_m \equiv \langle 0_1^+\|E2\|2_{1,\mathrm{ms}}^+\rangle$ and $\epsilon_f \equiv \langle 0_1^+\|E2\|2_f^+\rangle$, the observed $E2$ matrix elements are then given by

$$\langle 0_1^+\|E2\|2_3^+\rangle = -\beta\epsilon_m + \alpha\epsilon_f, \tag{17}$$

$$\langle 0_1^+\|E2\|2_4^+\rangle = \alpha\epsilon_m + \beta\epsilon_f. \tag{18}$$

Using the tabulated literature branching ratios $\Gamma_{2_3^+\to 2_1^+}/\Gamma_{2_3^+\to 0_1^+}$ and $\Gamma_{2_4^+\to 2_1^+}/\Gamma_{2_4^+\to 0_1^+}$ [23], and the $E2/M1$ multipole mixing ratios for the relevant decays, one can solve for the ratio ϵ_f/ϵ_m of $E2$ matrix elements to the ground state. The values we obtain from the observables and from the two-state mixing ratio r are $\epsilon_f/\epsilon_m = -0.66$ and $\epsilon_f/\epsilon_m = -1.8$. Both ratios are reasonable. More conclusive statements on the value of this ratio require lifetime information. Our point was to show that the strongly differing branching behavior of the $2_{3,4}^+$ states of ^{136}Ce is not in contradiction with an almost equal mixing of the unperturbed $2_{1,\mathrm{ms}}^+$ one-phonon configuration in both of these 2^+ states.

Although absolute transition strengths were not measured, one can make semiquantitative predictions for the transition strengths by making an assumption on the $M1$ matrix element, $\langle 2_1^+\|M1\|2_{1,\mathrm{ms}}^+\rangle$, which has been observed in other nuclei to be robust around 1 μ_N [8,9,11,14]. Assuming that $\langle 2_1^+\|M1\|2_{1,\mathrm{ms}}^+\rangle$ has a value of 1 μ_N, $B(M1)$ and $B(E2)$ values for transitions from the 2_3^+, 2_4^+, $2_{1,\mathrm{ms}}^+$, and 2_f^+ states to the 2_1^+ and 0_1^+ states can be calculated from the known branching ratios and the calculated mixing coefficients, α and β. This has been done for the solution $\epsilon_f/\epsilon_m = -1.8$ and the results are summarized in Table II. This estimate can be important for the design of Coulomb excitation experiments like the one previously done for ^{138}Ce [14].

TABLE II. Semiempirical predictions for transition strengths assuming $\langle 2_1^+\|M1\|2_{1,\mathrm{ms}}^+\rangle = 1\ \mu_N$.

	2_3^+	2_4^+	$2_{1,\mathrm{ms}}^+$	2_f^+
$B(M1;2_i^+\to 2_1^+)$	0.09 μ_N^2	0.11 μ_N^2	0.20 μ_N^2 [a]	–
$B(E2;2_i^+\to 2_1^+)$	2.9 W.u.	2.5 W.u.	0.0 W.u.[a]	5.4 W.u.
$B(E2;2_i^+\to 0_1^+)$	5.4 W.u.	0.34 W.u.	1.3 W.u.	4.5 W.u.

[a]This value has been assumed from systematics.

Last, we present our hypothesis for the nature of the 2_f^+ state as a predominantly three-phonon state and see whether available data support it. If there is three-phonon character in the 2_f^+ one would expect that there exist collective $E2$ transitions from the $2_{3,4}^+$ states to the lower lying two-phonon multiplet: (0_2^+), 2_2^+, and 4_1^+. In the literature, there are observations of $2_3^+ \to 2_2^+, (0_2^+)$ transitions and $2_4^+ \to 2_2^+, 4_1^+$ transitions, though the placement of the γ rays in the level scheme for the transitions to the 0_2^+ and 4_1^+ states are uncertain [23]. If the literature values were correct they would yield $\frac{B(E2;2_3^+\to 0_2^+)}{B(E2;2_3^+\to 2_1^+)} = 4.1(15)$ and $\frac{B(E2;2_4^+\to 4_1^+)}{B(E2;2_4^+\to 2_1^+)} = 3.3(12)$, respectively. We did not find evidence for the $2_3^+ \to (0_2^+)$ transition in our data set and observation of the $2_4^+ \to 4_1^+$ transition was beyond our data set's sensitivity. Therefore, we hesitate in using the published data for these transitions as proof for the three-phonon nature of the 2_f^+ state. The two decays to the 2_2^+ state from the $2_{3,4}^+$ states are seen in our data, but insufficient statistics prevent us from measuring multipole mixing ratios. Nevertheless, it is interesting to check whether the corresponding transition rates are large enough for the three-phonon hypothesis for the 2_f^+ state. From decay intensities to the 2_2^+ state relative to those to the 0_1^+ and 2_1^+ states we determine upper limits for the $E2$ branching ratios to the 2_2^+ state. This can indicate whether or not the current data rule out the possibility for large $B(E2)$ values to the two-phonon multiplet. The calculated ratios are

$$\frac{B(E2;2_3^+\to 2_2^+)}{B(E2;2_3^+\to 0_1^+)} \leqslant 4.9(7),$$

$$\frac{B(E2;2_3^+\to 2_2^+)}{B(E2;2_3^+\to 2_1^+)} \leqslant 9.1(31),$$

$$\frac{B(E2;2_4^+\to 2_2^+)}{B(E2;2_4^+\to 0_1^+)} \leqslant 21(3),$$

$$\frac{B(E2;2_4^+\to 2_2^+)}{B(E2;2_4^+\to 2_1^+)} \leqslant 2.9(11).$$

These upper limits are consistently greater than one. This shows that the currently known branching ratios are not in conflict with our hypothesis that the 2^+_f state is of predominantly three-phonon character.

V. CONCLUSION

Five previously unknown $E2/M1$ multipole mixing ratios were measured for five transitions between low-spin states populated by β decay in ^{136}Ce. Spin assignments for three states were confirmed for previously known assignments and two were newly assigned for tentative assignments. Positive parities were assigned for two states with unknown or tentative parity assignments based on the significantly large value for the $E2/M1$ multipole mixing ratios measured from the transitions from these states to states of known positive parity. Measured δ_1 values yielding $E2$ fractions of 0.17(5) and 0.14(5) for transitions to the 2^+_1 state from the 2^+_3 and 2^+_4 states, respectively, show a predominant $M1$ character. This suggests the 2^+_3 and 2^+_4 states to be fragments of the $2^+_{1,\mathrm{ms}}$ one-phonon mixed-symmetry state. Though the δ_1 values show a predominant $M1$ character, it does not give the absolute $M1$ strengths of the transitions, which are the signature of a mixed-symmetry state. Measurement of the absolute strengths is still needed.

The fact that ^{136}Ce had two closely spaced 2^+ states, namely, the 2^+_3 and 2^+_4 states, allowed for the F-spin mixing matrix element V to be estimated from a two-state mixing scenario where the $2^+_{1,\mathrm{ms}}$ state mixes with a closely lying fully-symmetric 2^+_f state. The value obtained from this calculation was $V = 43(5)$ keV supporting the recently introduced mechanism of shell stabilization of mixed-symmetry structures found in the neighboring isotope ^{138}Ce.

ACKNOWLEDGMENTS

We thank Richard Lefferts and Bruce Gutchow for the preparation of the ^{6}Li beam, Andre Lipski for the production of the ^{134}Ba targets, and Blagovest Botchev for assisting us in the construction of the irradiation chamber. We also thank Jan Jolie for the loan of the Stony Brook Cube spectrometer frame and target chamber. This research was supported by NSF Grant PHY 0245018 and by DOE Grant DE-FG02-04ER41334 and was partially supported by Bulgarian NSF Contract VUF05/06.

[1] F. Iachello, Phys. Rev. Lett. **53**, 1427 (1984).
[2] F. Iachello and A. Arima, *The Interacting Boson Model* (Cambridge University Press, Cambridge, 1987).
[3] T. Otsuka, A. Arima, and F. Iachello, Nucl. Phys. **A309**, 1 (1978).
[4] D. Bohle, A. Richter, W. Steffen, A. E. L. Dieperink, N. Lo Iudice, F. Palumbo, and O. Scholten, Phys. Lett. **B137**, 27 (1984).
[5] W. D. Hamilton, A. Irbäck, and J. P. Elliott, Phys. Rev. Lett. **53**, 2469 (1984).
[6] N. Pietralla, C. Fransen, D. Belic, P. von Brentano, C. Frießner, U. Kneissl, A. Linnemann, A. Nord, H. H. Pitz, T. Otsuka *et al.*, Phys. Rev. Lett. **83**, 1303 (1999).
[7] V. Werner, D. Belic, P. von Brentano, C. Fransen, A. Gadea, H. von Garrel, J. Jolie, U. Kneissl, C. Kohstall, A. Linnemann *et al.*, Phys. Lett. **B550**, 140 (2002).
[8] G. Molnár, R. A. Gatenby, and S. W. Yates, Phys. Rev. C **37**, 898 (1988).
[9] B. Fazekas, T. Belgya, G. Molnár, and Á. Veres, Nucl. Phys. **A548**, 249 (1992).
[10] J. R. Vanhoy, J. M. Anthony, B. M. Haas, B. H. Benedict, B. T. Meehan, S. F. Hicks, C. M. Davoren, and C. L. Lundstedt, Phys. Rev. C **52**, 2387 (1995).
[11] N. Pietralla, D. Belic, P. von Brentano, C. Fransen, R.-D. Herzberg, U. Kneissl, H. Maser, P. Matschinsky, A. Nord, T. Otsuka *et al.*, Phys. Rev. C **58**, 796 (1998).
[12] P. Van Isacker, K. Heyde, J. Jolie, and A. Sevrin, Ann. Phys. (NY) **171**, 253 (1986).
[13] A. Giannatiempo, A. Nannini, and P. Sona, Phys. Rev. C **58**, 3316 (1998).
[14] G. Rainovski, N. Pietralla, T. Ahn, C. J. Lister, R. V. F. Janssens, M. P. Carpenter, S. Zhu, and C. J. Barton, III, Phys. Rev. Lett. **96**, 122501 (2006).
[15] R. Wirowski, Ph.D. thesis, Universität zu Köln, 1993.
[16] H. Frauenfelder and R. M. Steffen, in *α-, β-, and γ-ray Spectroscopy*, edited by K. Siegbahn (North-Holland, Amsterdam, 1965), Vol. 2, Chap. XIXA, pp. 997–1198.
[17] K. S. Krane, R. M. Steffen, and R. M. Wheeler, Nucl. Data Tables **11**, 351 (1973).
[18] A. Bohr and B. Mottelson, *Nuclear Structure* (Benjamin, New York, 1969), Vol. I, Chap. 3C-2, pp. 380–383.
[19] L. C. Biedenharn and M. E. Rose, Rev. Mod. Phys. **24**, 249 (1953).
[20] R. M. Steffen and K. Adler, in *The Electromagnetic Interaction in Nuclear Physics*, edited by W. D. Hamilton (North-Holland, Amsterdam, 1972), Chap. XII.
[21] I. Wiedenhöver, O. Vogel, H. Klein, A. Dewald, P. von Brentano, J. Gableske, R. Krücken, N. Nicolay, A. Gelberg, P. Petkov *et al.*, Phys. Rev. C **58**, 721 (1998).
[22] I. Wiedenhöver (unpublished).
[23] A. A. Sonzogni, Nucl. Data Sheets **95**, 837 (2002).
[24] A. Gade, I. Wiedenhöver, M. Luig, A. Gelberg, H. Meise, N. Pietralla, V. Werner, and P. von Brentano, Nucl. Phys. **A673**, 45 (2000).
[25] S. Raman, C. W. Nestor Jr., and P. Tikkanen, At. Data Nucl. Data Tables **78**, 1 (2001).
[26] N. Pietralla, P. von Brentano, A. Gelberg, T. Otsuka, A. Richter, N. Smirnova, and I. Wiedenhöver, Phys. Rev. C **58**, 191 (1998).